A New Approach to Calculating Endurance in Electric Flight and Comparing Fuel Cells and Batteries

Link sito dell'editore:

https://www.sciencedirect.com/science/article/abs/pii/S0306261916317317

Link codice DOI: https://doi.org/10.1016/j.apenergy.2016.11.100

Citazione bibliografica dell'articolo:

Teresa Donateo, Antonio Ficarella, Luigi Spedicato, Alessandro Arista, Marco Ferraro, "A new approach to calculating endurance in electric flight and comparing fuel cells and batteries", pubblicato in Applied Energy, 2017, Volume 187,Pages 807-819

A New Approach to Calculating Endurance in Electric Flight and Comparing Fuel Cells and Batteries

Teresa Donateo, Antonio Ficarella, Luigi Spedicato
Department of Engineering for Innovation
University of Salento, Italy

Alessandro Arista, Marco Ferraro
Consiglio Nazionale delle Ricerche
Istituto di Tecnologie Avanzate per l'Energia "Nicola Giordano"
Messina, Italy

Corresponding author

Prof. Teresa Donateo
Department of Engineering for Innovation
Università del Salento, Lecce, Italy
Via per Arnesano, 73100 Lecce
Phone number: +39 0832 297 754
e-mail: teresa.donateo@unisalento.it

A New Approach to Calculating Endurance in Electric Flight and Comparing Fuel Cells and Batteries

Teresa Donateo, Antonio Ficarella, Luigi Spedicato
Department of Engineering for Innovation
University of Salento, Italy

Alessandro Arista, Marco Ferraro
Consiglio Nazionale delle Ricerche
Istituto di Tecnologie Avanzate per l'Energia "Nicola Giordano"
Messina, Italy

Abstract

Electric flight is of increasing interest in order to reduce emissions of pollution and greenhouse gases in the aviation field in particular when the takeoff mass is low, as in the case of lightweight cargo transport or remotely controlled drones.

The present investigation addresses two key issues in electric flight, namely the correct calculation of the endurance and the comparison between batteries and fuel cells, with a mission-based approach. As a test case, a light Unmanned Aerial Vehicle (UAV) powered exclusively by a Polymer Electrolyte Membrane fuel cell with a gaseous hydrogen tank was compared with the same aircraft powered by different kinds of Lithium batteries sized to match the energy stored in the hydrogen tank. The mass and the volume of each powertrain were calculated with literature data about existing technologies for propellers, motors, batteries and fuel cells. The empty mass and the wing area of the UAV were amended with the mass of the proposed powertrain to explore the range of application of the proposed technologies.

To evaluate the efficiency of the whole powertrain a simulation software was used instead of considering only level flight. This software allowed an in-depth analysis on the efficiency of all

sub-systems along the flight. The secondary demand of power for auxiliaries was taken into account along with the propulsive power.

The main parameter for the comparison was the endurance but the takeoff performance, the volume of the powertrain and the environmental impact were also taken into account. The battery-based powertrain was found to be the most suitable for low-energy applications while the fuel cell performed better when increasing the amount of energy stored on board. The investigation allowed the estimation of the threshold above which the fuel cell based powertrain becomes the best solution for the UAV.

1. Introduction

The reduction of pollutants and greenhouse gases emissions from aircraft is a topic of increasing interest. Even if air travel accounts for 2% of global CO_2 emissions, this proportion is set to grow in the future [1]. The industry is reliant on a selection of measures to contribute to reduce emissions [2] - [3] amongst which is the increased use of electricity.

Battery based and fuel-cell powertrains are used either as auxiliary power units for aircraft or as an electric propulsion system, for small Unmanned Aerial Vehicles (UAVs) [4]-[5].

Unmanned aircraft are used in a variety of military, homeland security, and civilian applications. Electric propulsion is preferred for its advantages: quiet operation, higher safety, precise power management and control.

Recently, a certain number of fuel-cell powered small unmanned UAVs and transport airplanes have been tested [6]-[9] . Hydrogen is a clean-burning fuel that produces heat and electricity if combined with oxygen with only water vapor as a by-product (from a tank-to-wing point of view). However, hydrogen is not an energy source but an energy carrier obtained by other sources of energy, such as reforming natural gas or by water electrolysis. Indirect pollution and greenhouse gas emissions should be carefully evaluated [10] to assess the well-to-wing environmental impact of hydrogen aircraft. Fuel cell systems are able to

guarantee high specific energy as well as high efficiency and so they prove to be convenient in some aeronautical applications [11].

Several types of fuel cells with different electrolytes can be used to power aircraft and they can require compressed or liquefied hydrogen. Polymer Electrolyte Membrane (PEM) fuel cells are the most commonly used and are appropriate for the application to UAV owing to their small size and their light weight [12] -[21]. For this reason they were chosen the test case considered in the present investigation to explain the proposed procedure.

Most studies on fuel cells applied to aircraft are exclusively conceptual. Only few works considers the usage of fuel cells on light or ultra-light aircraft [15]-[21] where battery-based powertrains are usually preferred. However, batteries have many drawbacks, the main being the limited values of power and energy density, that is the power and energy per unit mass and volume. These aspects discourage the use of batteries in heavier aircraft. In addition, the capacity and the life time of batteries are affected by many factors like discharge and recharge currents, operating temperature, etc. [20]. New battery technologies are under development but the present investigation focuses on Lithium batteries because they are the most commonly used for electric powered aircraft, are mass produced and readily available [22]. Battery-based powertrains also allow zero emissions from tank-to-wing point of view and, in addition, avoid the emission of water vapor in the atmosphere.

Recently, some efforts have been dedicated to the comparison between the two available technologies (batteries and fuel cells) for electric flight [23]-[25]. The comparison requires a correct estimation of electric endurance and must take into account the amount of energy stored on board. Note that the battery system stores energy in form of electricity while in the case of PEM fuel cells, energy is stored in form of compressed gaseous fuel.

For conventional powertrains, thermal engines burning liquid fossil fuels , the amount of energy on board is not a key issue because of the very high gravimetric and volumetric

density of liquid fuel [22]. For these systems the endurance is usually evaluated in conditions of level flight using the well-known Breguet formulas [26].

Breguet formulas can be used for fuel cell-based powertrain but not for the battery-based one, because the dependence of battery capacity on the discharge current makes it difficult to establish the actual energy available during the flight. Moreover, the concept of overall efficiency is meaningless because of the complexity of the charge/discharge processes.

Traub [27] proposed a formula to evaluate the endurance of battery-based powertrains in level flight that was corrected and validated experimentally in [28]. Another correction was proposed by Avanzini et al. [29] that underlined the increasing of the battery during level flight to compensate the reduction of voltage.

In the present investigation, a new approach is proposed to evaluate the efficiency of an electric aircraft. This approach is derived from the automotive field where it is a common practice to compare different drive trains on the same driving cycle [30], i.e. a series of data points representing the speed of a vehicle versus time. To apply the method to the aircraft field, a "mission" is defined as a series of data points representing the speed and the altitude of the aircraft versus time. At any point, the efficiency is evaluated by using detailed models for each powertrain sub-system. In particular, an efficiency map is used for the propeller while the fuel cell and the batteries are simulated with electrical equivalent circuit network models, that are characterized by simplicity, speed and acceptable accuracy [31]-[32].

The endurance calculated at level flight will be henceforward referred to as Gross Endurance (GE) while the terms Net Endurance (NE) will be used for the endurance evaluated with the proposed method.

The investigation consists of three parts. The first describes the proposed mission-based approach. In the second part the Gross and Net Endurances of a battery-based and a fuel-cell based UAV are analyzed over two different missions with an initial content of energy on-

board of about 2 MJ. The takeoff performance and the environmental impact of the proposed powertrains was also taken into account.

In the third part of the investigation, the energy on board is increased up to five times the initial value and the gross endurance is used to define a threshold above which the fuel cell based powertrain becomes the best solution for the electric UAV.

1 Specification of the UAV and modeling approach

In the present investigation the authors considered, as test case, a small and light UAV whose specifications were derived from literature [21] and reported in Table I.

Table I – Specification of the aircraft [21]

Aircraft specifications	*value*
Wing area [dm²]	188
Aspect ratio	23
Wing span [m]	6.58
Tail area [dm²]	45.5
Length from nose to tail [m]	2.38
Static thrust/weight	0.165
Wing airfoil	SD-7032
Airframe mass [kg]	7.4

Two virtual powertrain were considered (see Figure 1). The propeller and the electric motor were assumed to be the same for both cases.

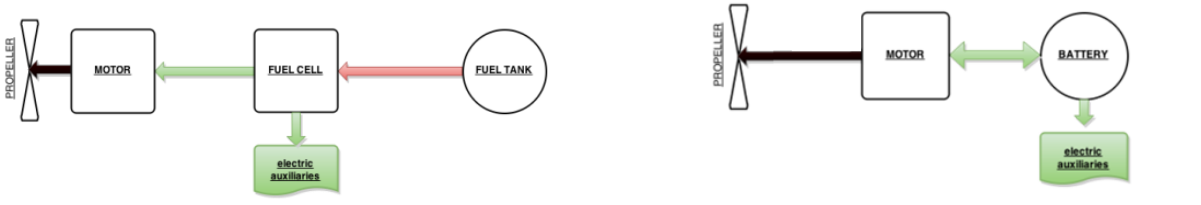

a) Fuel cell based powertrain

b) Battery-based powertrain

Figure 1 – The proposed powertrains

The propeller considered in the present investigation is a 22×10 APC E. The mass of the propeller is 169 g [33] and its speed was set equal to 3000 rpm in the simulations. The efficiency was calculated with a performance map as explained later.

For the aim of selecting an electric motor for the aircraft, the authors made use of *Drive Calculator 3.4*, an on-line tool to match motors and propellers [34]. Among the several electric motors compatible with the propeller , the Hacker C50-10 L Acro Competition brushless motor was chosen because of its low weight, small size and long life [35]. The selected electric

motor has a mass of only 423 g, including the gearbox. It was equipped with a Spin Master 125-opto controller whose mass is 160 g. The Spin Master 125-opto controller needs an operating voltage from 12 V to 50 V and it is directly connected to the motor in order to provide the required current and voltage.

This gear is incorporated into the Hacker motor C50-10 L Acro Competition and it assures a 6.7:1 reduction between the motor axis and the propeller axis [35].

1.1 The fuel-cell based powertrain

The demonstrator UAV found in literature [21] has a fuel-cell based powertrain with a 500 W 32-cell self-humidified hydrogen-air PEM fuel cell.

The hydrogen tank consists of a carbon fiber/epoxy cylinder with a capacity of 192 Standard liters (about 17g). Assuming the Lower Heating Value (LHV) of Hydrogen equal to 0.12 MJ/g, the energy stored on board with the 192 SL tank is equal to 1.93 MJ.

The characteristics of the fuel cell and the hydrogen tank are summarized in Table II [21].

The same PEM fuel cell and the same storage system was considered in the present investigation.

Table II – Specification of fuel cell and hydrogen tank

Specification	*value*
Number of cells	32
Cell area [cm^2]	64
Working temperature [K]	333.15
Storage pressure [MPa]	31
Storage capacity [SL]	192
Peak output power [W]	465
Specific electrical power [W/kg]	52
Specific electrical energy [Wh/kg]	7.1

1.2 The battery-based powertrain

Three different technologies [36] were considered for the battery-based powertrain: Lithium Iron Phosphate (LiFePO4), Lithium Polymer (LiPo) and Nickel Based Cathode (LiFP6) . Their specifications are shown in Table III.

To reach the same content of energy of the fuel-cell based powertrain (1.93 MJ), the nominal capacity of the battery was set equal to 13Ah for all technologies while the number of elements in series was adjusted as in Table III.

Table III – Specifications of the batteries

Type	Rated capacity C_{nom} [Ah]	Peak current [A]	Max continuous discharge current [A]	Peukert coefficient	Single battery voltage V [V]	Number of elements in series N_b	Bus voltage V_{bus} [V]
LiFePO4	13	130.0	39.0 (3C)	1.005	3.2	12	38.4
LiPo	13	130.0	65.0 (5C)	1.050	3.7	11	40.7
LiFP6	13	71.5	28.6 (2.2C)	1.300	3.6	11	39.6

The actual battery energy content E_b (in MJ) is equal to 1.80 MJ for the LiFePO4 battery pack, 1.90 MJ for the LiPo battery pack and it is equal to 1.85 MJ for the LiFP6 case.

1.3 The missions

The flight level and the true airspeed (TAS) time histories considered in the present investigation are depicted in Figure 2 and Figure 3 . Two different missions named “smooth” and “rough” respectively were considered. The “smooth” mission is a typical flight profile for an aircraft, based on the rate of climb, cruise speed and rate of descent derived from [21]. The “rough” mission was considered to simulate real world flight conditions for small drones. In particular, the “rough” mission was obtained from the “smooth” one by adding a disturbance with the same amplitude and frequency of the portion of experimental mission found in [21]. Points A-D in Figure 2 and Figure 3 will be used to underline the variability of the propeller efficiency in the following section.

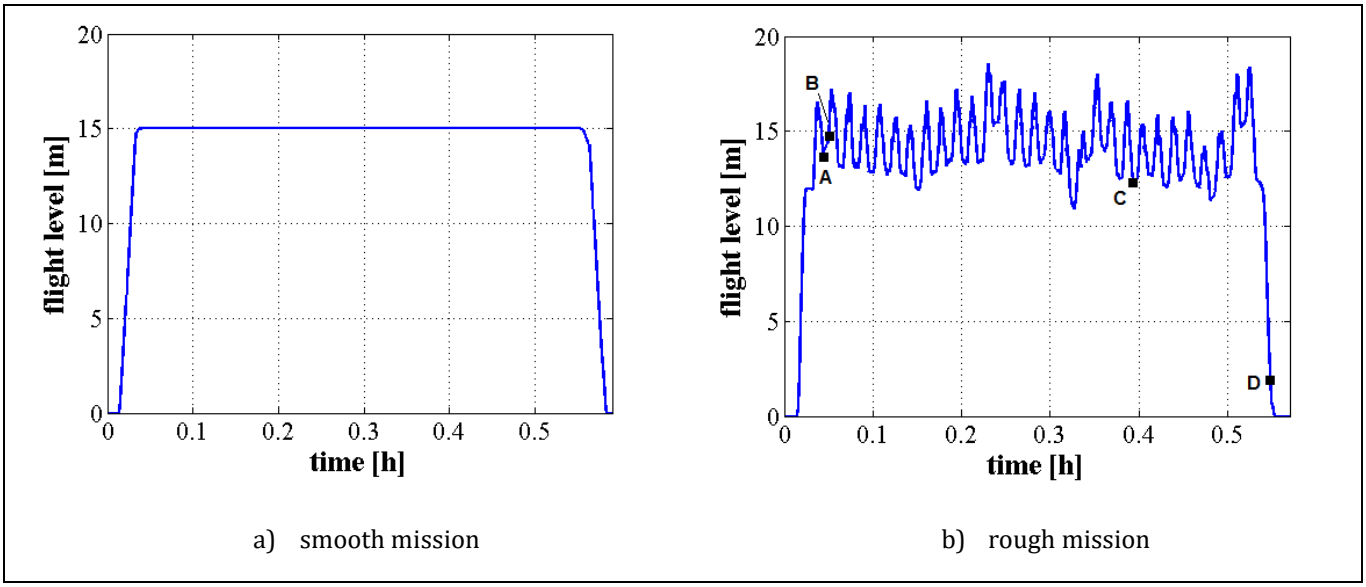

a) smooth mission b) rough mission

Figure 2 – Flight level vs time for the proposed missions

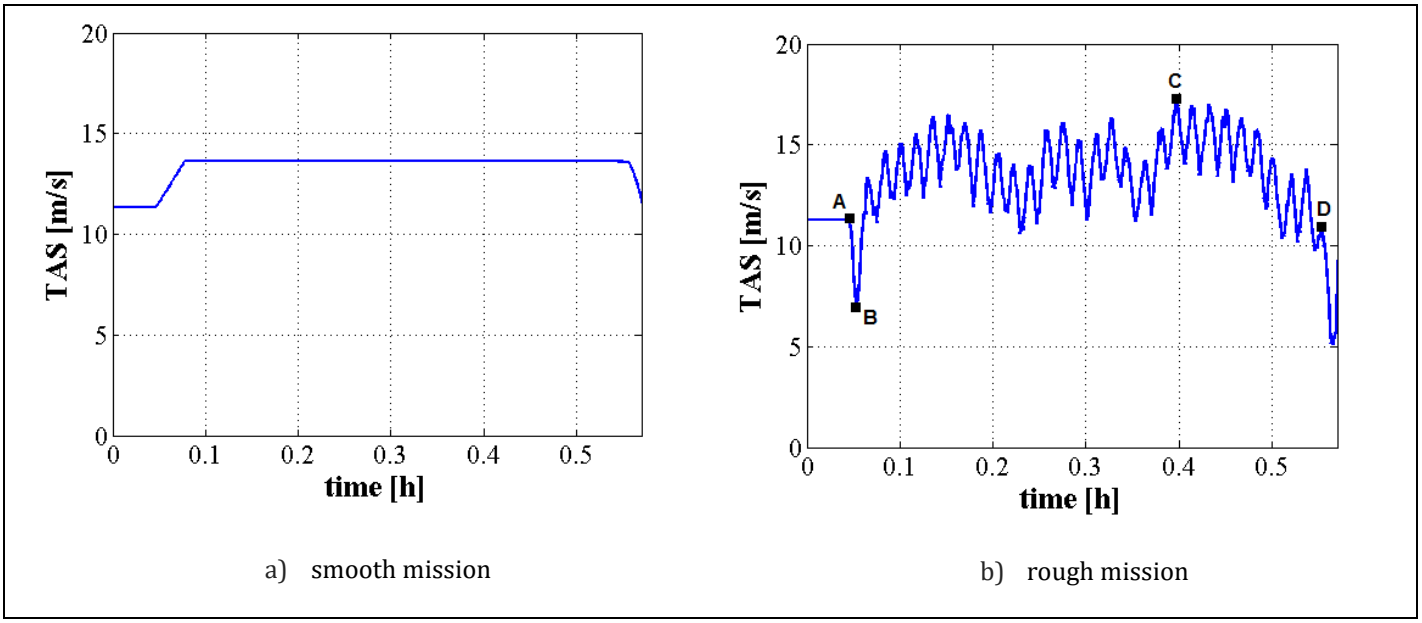

a) smooth mission b) rough mission

Figure 3 – True Air Speed (TAS) vs time for the proposed missions

1.4 Modeling the energy flows in the powertrain

The energy flows in the proposed powertrains were calculated with PLA.N.E.S., an in-house simulation and optimization software for conventional and innovative powertrains for aircraft [37]-[39]. Detailed information about the simulation code and its validation can be found in [38].

The PLA.N.E.S. software uses a backward simulation approach, i.e. the time histories of speed (V) and altitude (z) are used to calculate, at any time step, the thrust power to be delivered by the powertrain.

The thrust (T) is obtained by considering the equations of motion normal and along the flight path [26]:

$$L = W\cos\gamma - \frac{W}{g}\ V\ \frac{d\gamma}{dt} = \frac{1}{2}c_L\rho S V^2 \tag{1}$$

$$T = D + W\sin\gamma + \frac{W}{g}\ \frac{dV}{dt} + \mu W \tag{2}$$

Where γ is flight path angle and the drag force can be written as:

$$D = \frac{1}{2}c_D\rho S V^2 \tag{3}$$

W is the weight of the aircraft, c_L is the lift coefficient, ρ is the air density at the current flight level, g is the gravity constant, S is the wing area. The flight path angle is obtained by the mission profile as:

$$\sin\gamma = \frac{V}{dz/dt} \tag{4}$$

The rolling force μW depends on the friction coefficient μ and it is zero in flight while the gravitational force $W\sin(\gamma)$ is zero in level flight.

The drag polar is expressed by:

$$c_D = c_{D0} + \frac{S}{\pi \cdot b^2 \cdot \mathrm{e}}c_L{}^2 \tag{5}$$

where c_{D0} is the zero lift drag coefficient, b is the wing span and e is the Oswald's efficiency factor. The values of e (0.8) and c_{D0} (0.019) were assumed as suitable values for small UAVs [40], [41]. They were verified by applying the proposed simulation model on the recorded flight conditions of [21] and comparing the resulting power request with the data reported in [21].

When the airplane is powered by fuel, the fuel consumption entails a mass variation with respect to the overall mass at the start of mission. However, this effect is negligible for the proposes fuel cell powertrain because the mass of hydrogen is less than 0.5% of the takeoff mass for all the cases considered in the present investigation.

The required electric power P_{el} can be found from:

$$P_{el} = \frac{T \cdot V}{\eta_p \cdot \eta_{mot}} + P_{aux} \tag{6}$$

where P_{aux} is the electric auxiliary power, η_{mot} and η_p are the efficiencies of the motor and the propeller, respectively.

The electric auxiliary power (see Figure 4) was arbitrary assumed for lack of data. It was included in the investigation because it is important to underline that propulsive power is not the only request to be satisfied by the battery/fuel cell, particularly in the descent phase.

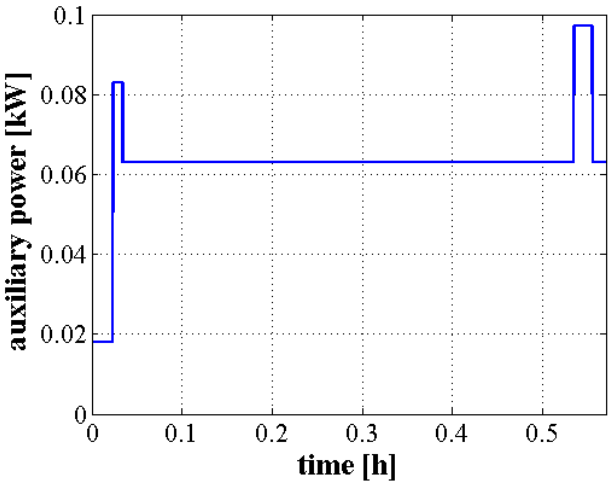

Figure 4 – Electric auxiliary power vs time for the proposed missions

1.4.1 The propeller sub-model

The propeller efficiency at any time along the mission is calculated by entering the performance map and interpolating the iso-efficiency lines (as in Figure 5). The map is entered by calculating the advance ratio *J*:

$$J = \frac{V}{nD} \tag{7}$$

and the thrust parameter C_T:

$$C_T = \frac{T}{\rho n^2 D^4} \tag{8}$$

Where V is the aircraft speed, n the propeller speed in rpm, D the propeller diameter, T the required thrust and ρ the air density

The propeller map was drawn from performance data available on the APC web site [33] and is reported in Figure 5 together with some working points along the "rough" mission to underline the variability of propeller efficiency .

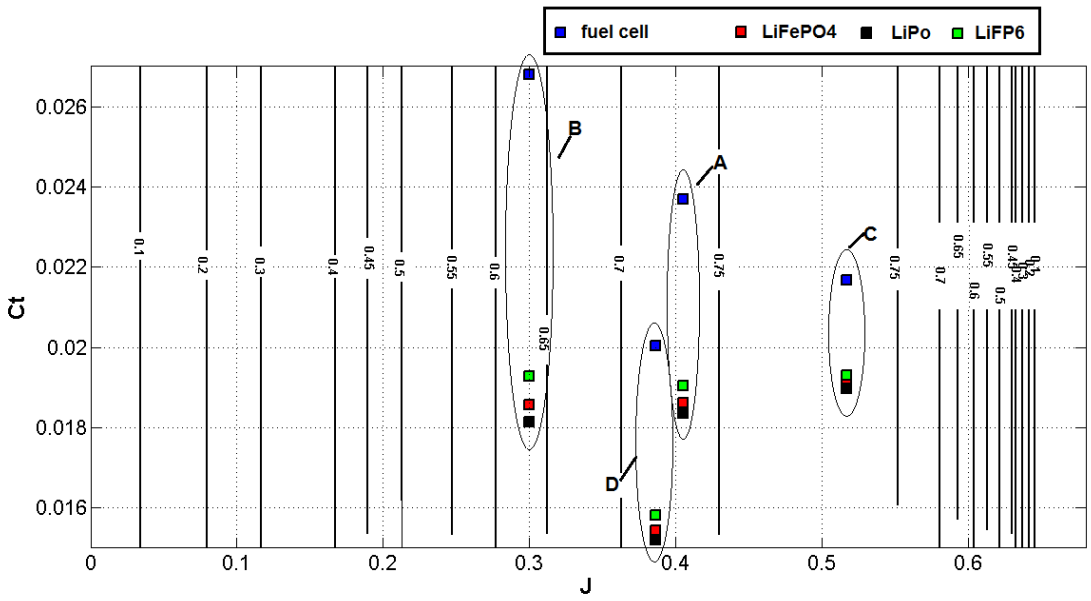

Figure 5 – Map of the propeller (contour lines=efficiency) and working points along the "rough" mission

For all the powertrain the efficiency increases from 0.1 at the beginning of takeoff (J=0) to 0.73 at the end of climb (point A) with an average of 0.55. During cruise efficiency changes continuously in the rough mission. For example, it is about 0.64 in point B and 0.75 in point C. In average it is 0.78 for all the powertrains. During descent and landing, the efficiency

decreases from 0.72 (point D) to 0.1 (J=0). The average values of efficiency will be used to calculate the gross efficiency.

1.4.2 The motor sub-model

The efficiency of the electric drive (motor and controller) was set equal to 0.9 in all points of the mission because a full performance map was not available. However, the proposed methodology is assumed to take into account the variability of motor efficiency with speed and torque [35].

The overall required electric power for propulsion and auxiliaries (see eq. 8) is given in Figure 6 for both the smooth and rough missions. For the battery-based powertrain, the figure shows only the results for LiFP6 because the curves for the other kinds of battery are almost identical.

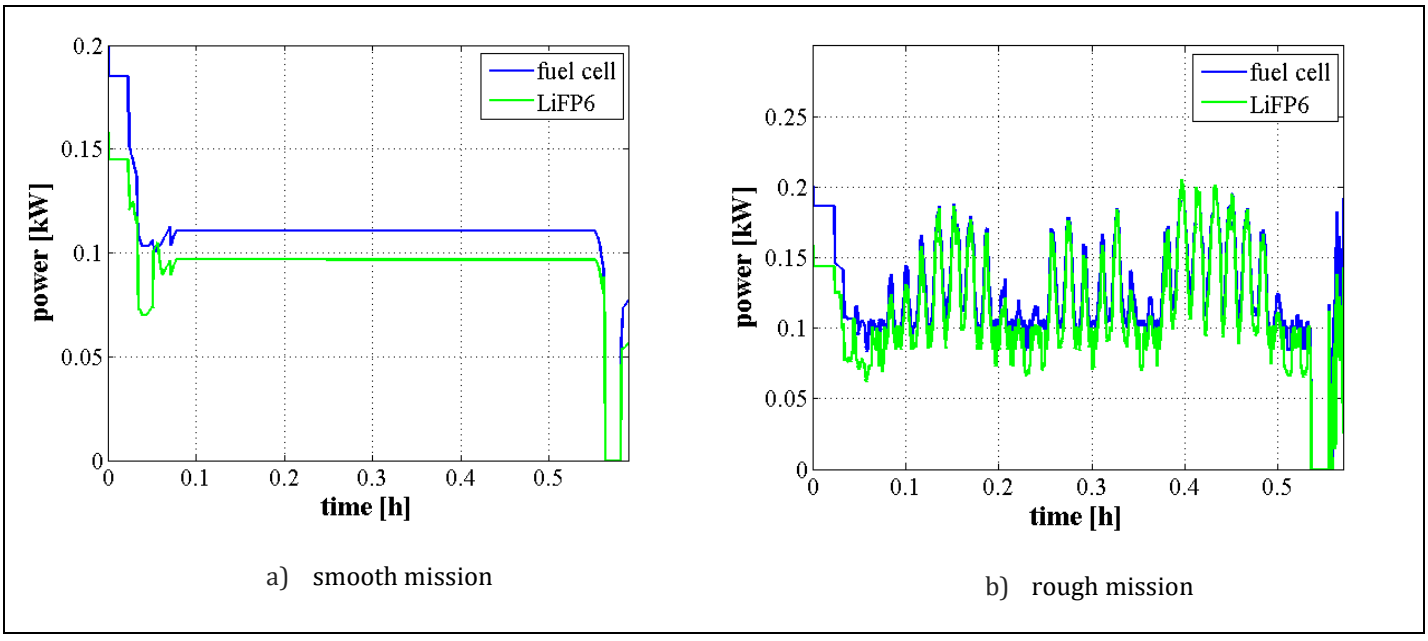

a) smooth mission

b) rough mission

Figure 6 – Electric power request vs time for the proposed missions

1.4.3 The fuel cell sub-model

The PEM fuel cell sub-model receives as input the electric power P_{el} and calculates the fuel cell current according to the number of cells n_{FC} and the cell area A_{FC} in cm^2 by inverting the following correlation proposed in literature[42]:

$$P_{el} = n_{FC} i_{FC} \cdot \left[E - r \cdot \frac{i_{FC}}{A_{FC}} - A \cdot \log\left(\frac{i_{FC}}{A_{FC} \cdot i_0} + \frac{i_n}{i_0} \right) - m \cdot e^{\frac{q \cdot n_{FC} i_{FC}}{A_{FC}}} \right] \quad (9)$$

where i_{FC} is in expressed in A, P_{FC} is expressed in W. The model parameters E, r, A, i_0, i_n, m and q were identified by minimizing the Euclidean distance with an experimental curve of the fuel cell tested in [42] that was very similar to that used in the present investigation.

The values found with the minimization procedure are given in Table IV.

Table IV – Estimated parameters of the fuel cell sub-model

Name	*E*	*r*	*A*	i_0	i_n	*M*	*q*
Unit	*[V]*	*[Ω/cm²]*	*[V]*	*[A/cm²]*	*[A/cm²]*	*[V]*	*[cm²/A]*
Value	0.953	0.389	0.01856	$3.22 \cdot 10^{-5}$	0.00045	$2.44 \cdot 10^{-5}$	7.22

The fuel cell efficiency η_{FC} (Figure 7) can be expressed as:

$$\eta_{FC} = \frac{2 \cdot F \cdot P_{FC}}{n_{FC} i_{FC} \cdot \Delta H} = \frac{0.6795 \cdot P_{FC}}{n_{FC} i_{FC}} \quad (10)$$

where F = 96485.4 C/mol is the Faraday constant and ΔH = 284000 J/mol is the chemical reaction energy.

The instantaneous hydrogen consumption Q_{FC} is directly proportional to the instantaneous current i_{FC} :

$$Q_{FC} = k \cdot n_{FC} \cdot i_{FC} \quad (11)$$

where Q_{FC} is expressed in kg/s, and k is $1.0262 \cdot 10^{-8}$ kg/(A·s).

The instantaneous consumption can be evaluated from the required electric power as in Figure 7. Note that the hydrogen fuel consumption is not linearly proportional to power because of the non-constant efficiency of the stack also shown in Figure 7.

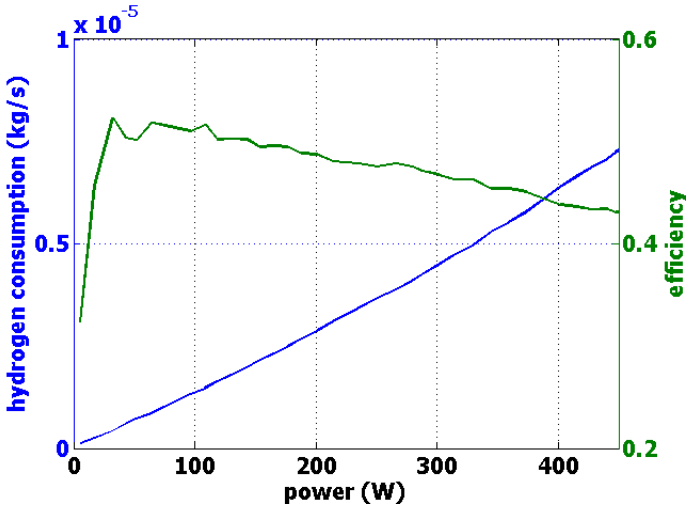

Figure 7 – Instantaneous consumption of hydrogen and fuel cell efficiency vs required power

Instantaneous fuel consumption and total hydrogen consumed in the two missions are given in Figure 8.

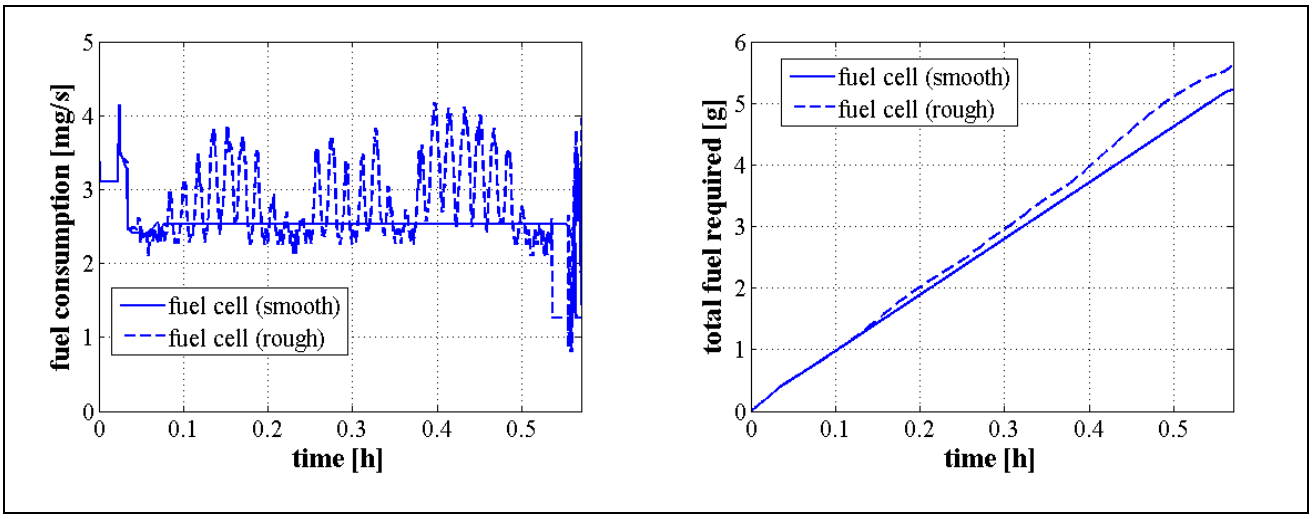

Figure 8 – Instantaneous hydrogen consumption and total required fuel along the proposed missions

In the "smooth" mission, the instantaneous hydrogen consumption has a maximum value of 4.17 mg/s at take-off and a steady consumption of 2.53 mg/s in cruise. In the "rough" mission, several high consumption peaks are found.

The total fuel consumption is about 5.42 g for the "smooth" mission and 5% larger for the rough mission.

The time history of the fuel cell current for the two missions is shown in Figure 9 together with the results of the battery powertrains. Note the large peak of required power at the end of the climb phase and the high frequency peaks during the descent in both missions.

The efficiency of the fuel cell is, on average, 0.43 at take-off and 0.52 at cruise. These values will be used to evaluate the gross efficiency of the fuel cell-based powertrain.

With the proposed model, the fuel cell is assumed to be able to follow the dynamic of the rough mission. However, this could not be the case in reality, the dynamic response being one of the drawback of the fuel cells due to hysteresis phenomena [43] that can be solved by considering a hybrid powertrain (i.e. by adding a battery).

1.4.4 The battery sub-model

The battery current I at time t is calculated from the power $P_{el}(t)$:

$$I(t) = \frac{P_{el}(t)}{V(t)} \tag{12}$$

To calculate the battery voltage $V(t)$, the battery is modelled as a voltage generator that is connected in series with a resistor, whose value R is equal to the battery internal resistance. The voltage V at time t is a function of the open circuit voltage V_{OC}, that, in turn, depends on the SOC (evaluated at the previous time step).

$$V(t) = V_{OC}(t) - R \cdot I(t) \tag{13}$$

As suggested by Tremblay et al.[44], the open circuit voltage is calculated as the sum of three terms: a constant voltage E_0, a polarization term and an exponential loss:

$$V_{OC}(t) = \mathrm{E}_0 - \frac{100 \cdot \mathrm{K}}{SOC(t-1)} + \mathrm{A} \cdot e^{-\mathrm{B} \cdot C_{nom}\left(1 - \frac{SOC(t-1)}{100}\right)} \tag{14}$$

The values of the parameters R, E_0, A, K and B depend on the battery technology and are reported in Table V for the selected battery technologies: LiFePO4, LiPo and LiFP6. These

parameters were obtained by comparison with experimental discharge curves [46] using the procedure proposed by Tremblay et al. [45].

Table V – Estimated parameters of the battery sub-model

	LiFePO4	LiPo	LiFP6
R (Ω)	0.0010	0.0010	0.0008
E_0 (V)	3.2	3.7	3.9
K (V)	0.00035	0.00078	0.00045
A (V)	0.4574	0.5458	0.3058
B ($(Ah)^{-1}$)	1.5000	0.1000	1.3569

The reduction of capacity when the battery is discharged at a current higher than the nominal current (equal to 1C) is a phenomenon widely studied in literature [46]-[51]. It was taken into account by introducing a pseudo-effective current I_{eff}, defined as proposed by [46].

$$I_{eff} = I\left(\frac{I}{I_{nom}}\right)^{n_b - 1} \tag{15}$$

where n_b is the Peukert coefficient that depends on the temperature, the concentration of the electrolyte and the structure of the batteries [46]-[51]. The values of the Peukert coefficient n_b are reported in Table III.

The electric current curves along the missions for the proposed powertrains are illustrated in Figure 9. The maximum value of current draw from the battery along the proposed missions is 8A. This corresponds to about 0.6 C and is below the maximum continuous discharge current for all the technologies (see Table III). Note that in the "smooth" mission, the power during the cruise phase is constant (Figure 6). Nevertheless, the battery current increases with time because the voltage drops with battery state of charge (see eq 16). This is particularly evident for the low-performance LiFePO4 battery and affects the aircraft endurance as explained later.

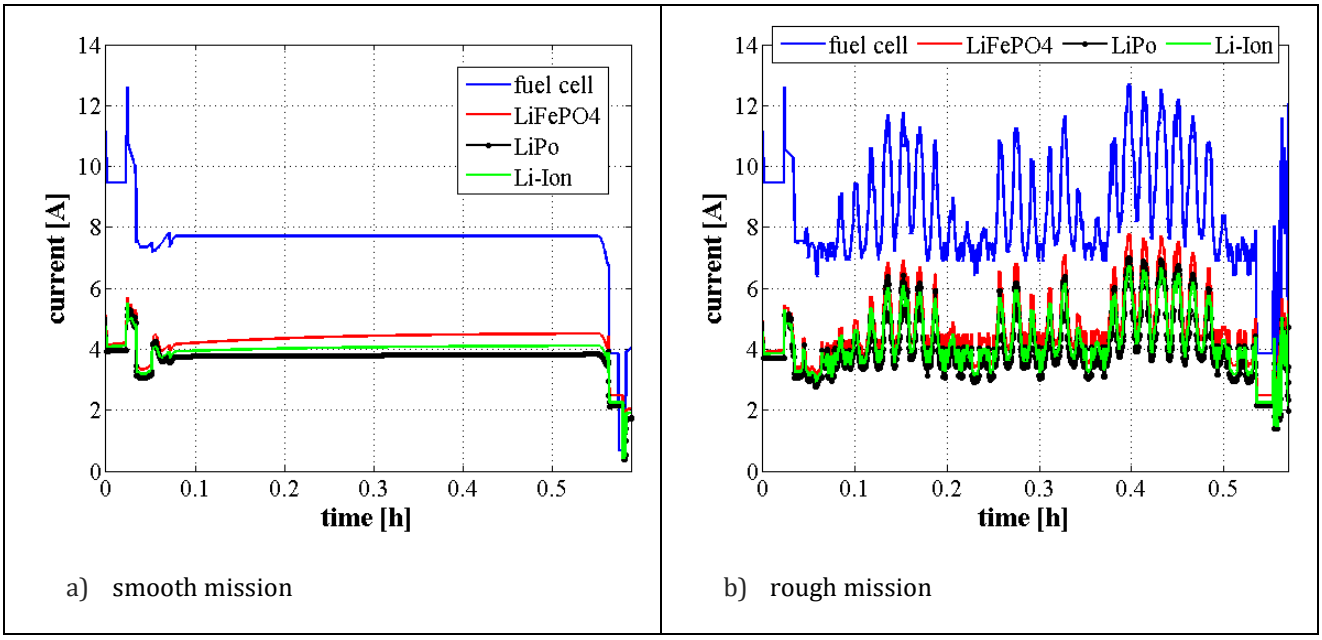

Figure 9 – Fuel cell and the battery currents versus time along the proposed missions

The actual state of the charge(*SOC*) of the battery at time t along the mission is calculated as:

$$SOC(t) = SOC(t - \Delta t) - 100 \cdot \frac{I_{eff}(t)}{C_{nom}} \Delta t \tag{16}$$

Along the proposed missions, the *SOC* decreases with time and the final value depends on battery typology and mission specification as shown in Figure 10.

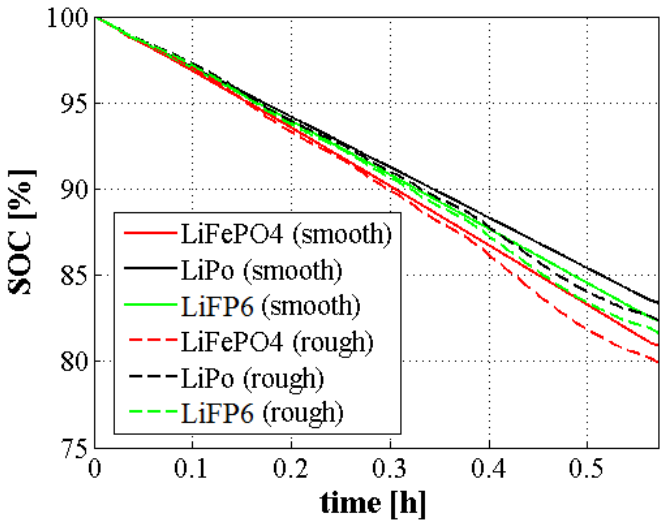

Figure 10 – State of Charge of the batteries vs time along the proposed missions

The final values of *SOC* values are lower in case of the rough mission because additional power is required to lead the aircraft back to the flight level when the altitude decreases as a consequence of the unstable flight.

2 Comparison of the powertrains with the initial energy content

The mass and the volume of the proposed powertrains when the energy content is 1.9MJ is shown in Table VI. The peak power is also reported. In the fuel cell powertrain, the power is limited by the fuel cell nominal power, while in the battery-based case it is limited by the motor peak power (600W).

Table VI – Specification of the proposed powertrains

Type	Energy source	Aircraft mass *m* (kg)	Powertrain mass (kg)	Powertrain volume (m^3)	Peak power at take-off [W]
PEM fuel cell and relating plant	hydrogen	16.6	9.2	0.0083	465
LiFePO4	electricity	12.9	5.5	0.0023	600
LiPo	electricity	12.7	5.3	0.0022	600
LiFP6	electricity	13.3	5.9	0.0035	600

The mass evaluation is essential to estimate correctly the performance of the powertrains.

At take-off the most important specification is the peak power per unit mass that affects the acceleration and the required runway length. From this point of view, the best solution is represented by the LiPo battery-based powertrain with 45 W/kg versus 28 W/kg for the fuel cell system.

At cruise, the most important parameter is the "overall efficiency" considered as the product of propeller, motor and power source efficiencies. The overall efficiency parameter influences endurance, fuel consumption and environmental impact.

The efficiency of the propeller and fuel cells at take-off and cruise were obtained from the results of PLA.NE.S as already explained. In concert with the (constant) efficiency of the motor, they allow the conversion losses of the powertrain to be calculated.

For the battery powertrain, the nominal energy efficiency of the three kinds of battery was considered to evaluate the "storage losses" [47].

The overall efficiency and the losses in the components of the powertrain are shown in Figure 11. The best powertrain is again the LiPo case with a total efficiency of 68% at cruise and 48% at takeoff; the worst one it the fuel cell powertrain with an average of 25.7% at takeoff and 30.2% in cruise. In the case of battery-based powertrain, the largest amount of losses are in the propeller because of the high efficiency of the other components while the conversion losses of the fuel cell itself are the most critical in the fuel cell-based powertrain.

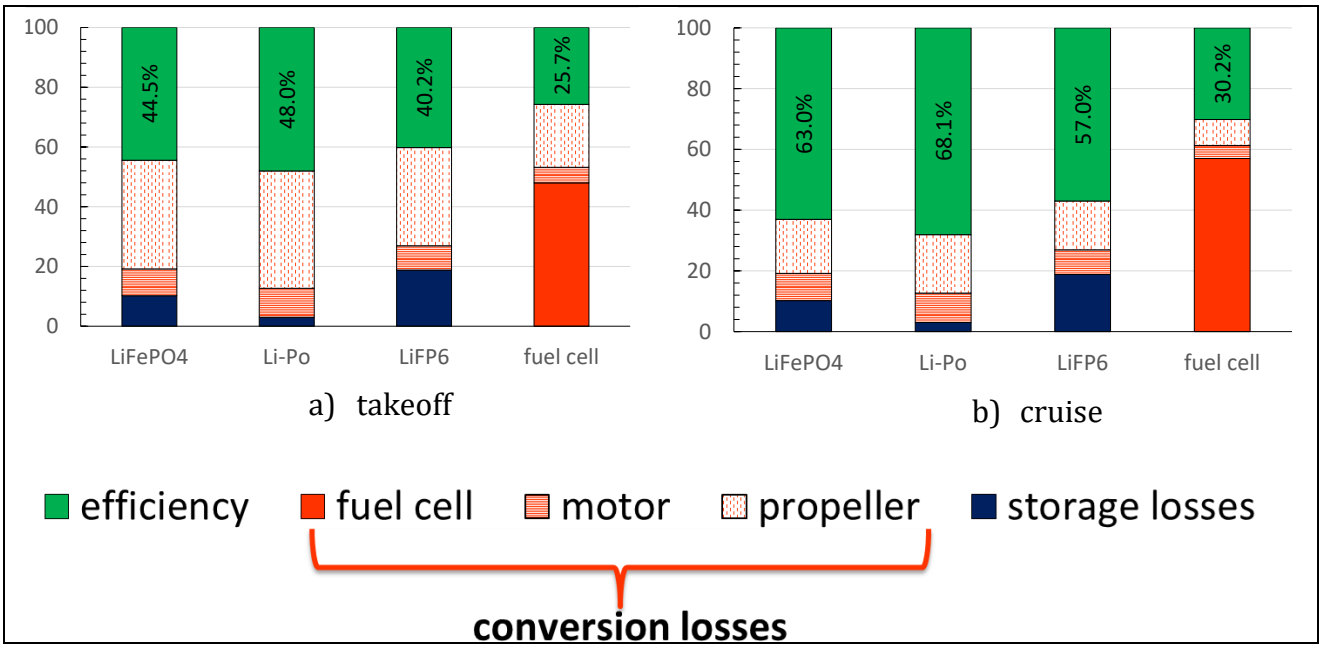

Figure 11- Energy balance of the proposed powertrain

2.1 Gross endurance

The endurance of the powertrain is an important design parameter for the UAV and depends on both the overall efficiency at cruise and the aircraft mass. Thus, the LiPo is expected to give the best results.

In case of batteries, the gross endurance E_{batt} in hours of an aircraft can be calculated as proposed in literature [26]:

$$E_{batt} = R_t^{1-n_b}\left(\frac{\eta_{tot} V_{bus} C_b}{P_{req}}\right)^{n_b} \tag{17}$$

where R_t is the battery hour rating, that is the discharge time over which the capacity is determined (1 h for all batteries analyzed in the present investigation). η_{tot} is the total efficiency at cruise (Figure 11), n_b is the Peukert coefficient (Table III) and P_{req} is the power required to overcome the drag. The power P_{req} is obtained by:

$$P_{req} = \frac{1}{2}\rho V^3 S c_{D0} + \frac{2W^2}{\pi b^2 e \rho V} \tag{18}$$

The endurance is maximum [26] when the speed V is equal to U_E :

$$U_E = \sqrt{\frac{2W}{\rho S}\sqrt{\frac{S}{3\pi b^2 e c_D}}} \tag{19}$$

Note that this approach considers the efficiency of the propeller constant and the battery voltage invariant (consequently the current drawn from the battery is also constant). Eq. (19) was validated experimentally and it was found to overestimate the electric endurance in level flight by 10-14% [28]. Some corrections to this approach have been proposed in literature ([28] ,[29]) . However, these works refer to level flight conditions and do not take into account the variability of power request in the whole mission that causes the battery current to change over and over again, as shown in (Figure 9).

In the case of the fuel cell, the hydrogen consumption is calculated from the required power P_{req} (Figure 7) and the gross endurance E_{FC} in hours is estimated by the ratio between the storage capacity C_{FC} in kg and the fuel consumption converted in kg/h (i.e. neglecting the variation of aircraft weight along the mission). The estimated maximum values of gross endurance are reported in Table VII together with the actual gross endurance, i.e. the endurance calculated at the actual cruise conditions (aircraft speed equal to 13.6 m/s).

Note that the best values of max endurance and range are obtained with the LiFP6 battery because of the highest value of the Peukert coefficient. Its gross endurance is 16% higher than in the case of LiPo. The performance of the fuel cell is quite poor with the reference value of energy stored on board (1.9 MJ). However, for the fuel cell, the max and actual gross

endurances differ only by 15%. This is because the best efficiency speed (6m/s) is closer to the cruise value (13.6m/s) than in the battery case (average value 5.1 m/s)

The differences among the different powertrains become less evident when the actual gross endurance is considered. In particular, the PEM fuel cell actual endurance is only 7% lower than that obtained with the LiPePO4 battery pack.

Table VII – Gross endurance and range of the proposed powertrains (1.9 MJ)

	PEM fuel cell	**LiFePO4 battery pack**	**LiPo battery pack**	**LiFP6 battery pack**
Max gross endurance (h)	4.8	6.4	8.2	9.5
Actual gross endurance (h)	4.1	4.4	5.4	6.0

2.2 Net endurance

The net endurance is calculated by extrapolating the results of PLA.N.E.S. along the proposed missions. In particular, for the battery-based case, the SOC curves of Figure 10 were prolonged up to fully discharge the batteries (SOC=20%). Similarly, the fuel consumption curves of Figure 8 were used to calculate the flight time at which the on-board hydrogen is consumed.

The mission based values of endurance are compared with the single point analysis gross endurance in Figure 12. Note that the LiPo battery gives the best results with the mission-based approach even if the difference with the LiFP6 is very small. However, the LiFP6 have a longer cycle life (3000 vs 800 of the LiPo battery) [47].

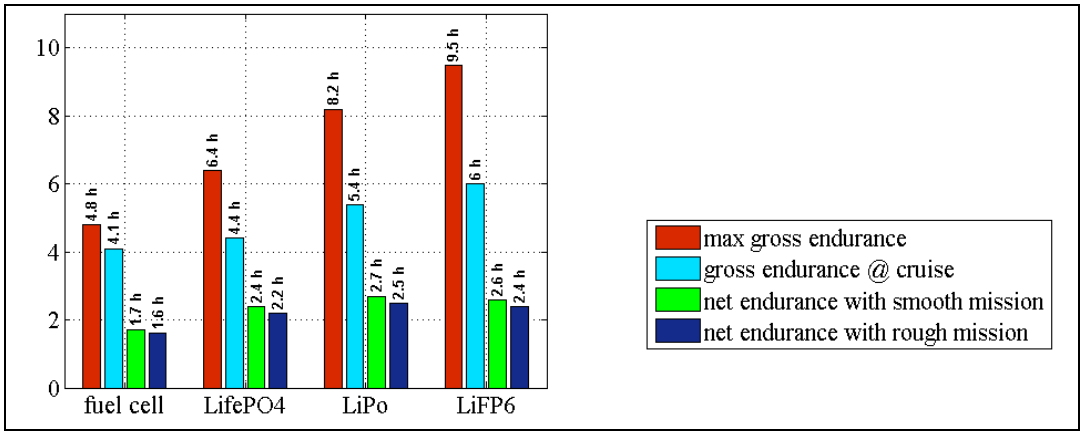

Figure 12 – Single point and mission-based endurance with the initial energy content

The presence of the disturbance in the rough mission determines a reduction of net endurance of about 8% for the battery-based powertrain and 6% for the fuel cell system. In average, the net endurances with the smooth and rough missions are, respectively, 47% and 44% of the actual gross endurance estimated with the correlations found in literature. To explain the difference between gross and net endurance, the overall propulsive mission efficiency η is calculated as the ratio between the required propulsive energy E_p and the energy consumption E_c:

$$\eta = \frac{E_p}{E_c} = \frac{\int_0^{\tau} T(t) \cdot V(t) dt}{E_c} \tag{20}$$

where τ is equal to the simulation duration.

In the case of batteries, the energy consumption is calculated as:

$$E_c = E_b \cdot \frac{\Delta SOC\ (\%)}{100} \tag{21}$$

where E_b is the battery energy content and ΔSOC (%) is the percentage difference between the initial and the final values of SOC. As the initial SOC is 100%, ΔSOC (%) is obtained by subtracting the final values of Figure 10 to 100 in all considered cases.

For the fuel cell-based powertrain, the energy consumption is calculated as:

$$E_c = E \cdot \frac{M_{FC}(\tau)}{C_{FC}} \tag{22}$$

in which E is the fuel cell energy content, $M_{FC}(\tau)$ is the consumed hydrogen and C_{FC} is the hydrogen storage capacity.

The comparison between the mission efficiency η and the single-point efficiency at take-off and cruise η_{tot} is given in Table VIII.

Table VIII – Propulsive efficiency of the proposed powertrain

	fuel cell	LiFePO4	LiPo	LiFP6
single-point efficiency at take-off	0.20	0.44	0.48	0.40
single-point efficiency at cruise η_{tot}	0.37	0.63	0.68	0.57
smooth mission efficiency η	0.28	0.41	0.44	0.44
rough mission efficiency η	0.26	0.40	0.43	0.44

Note that the mission-based efficiency is significantly lower than the single-point efficiency at cruise. This explains the results of Figure 12. On the other hand, the differences between the smooth and the rough mission are mostly due to the higher power request.

2.3 Environmental impact

The well-to-tank (WTT) emissions of the proposed powertrain depend on the energy mixing used to generate the electricity or the hydrogen fuel. In the case of batteries, WTT emissions are affected by the national electricity generation system. An average emission of 0.337 kg of CO_2 per kWh of electric energy was obtained in 2013 [52] in Italy. The differences in emissions among the different battery technologies are negligible because of the similar power request.

The emissions of CO_2 in the case of the fuel cell can be estimated by taking into consideration the possible options for hydrogen production, namely reforming and water electrolysis. In the reforming process, methane obtained from natural gas is heated with steam to produce a mixture of carbon monoxide and hydrogen. In the electrolysis case, a direct electric current is used to drive a chemical reaction. This process is highly inefficient because of the large amount of electricity required to split the water molecule. To obtain 1 g of H_2, 9.827 g of CO_2

are produced by the reforming process and 32.468 g of CO_2 are emitted on the air by the electrolysis process [53].

The Well–To-Wing emissions estimated for the two electric powertrains are shown in Figure 13. Note that CO_2 emissions are much greater when the powertrain is based on fuel cell particularly if hydrogen is obtained from electrolysis. However, this is a result related to the present Italian context. The environmental impact of both kind of powertrains is zero from a WTW point of view if renewable energy is used to recharge the battery or for the electrolysis. Emissions associated to manufacturing and disposal are important for both powertrains but they were neglected in the present investigation [54]-[55].

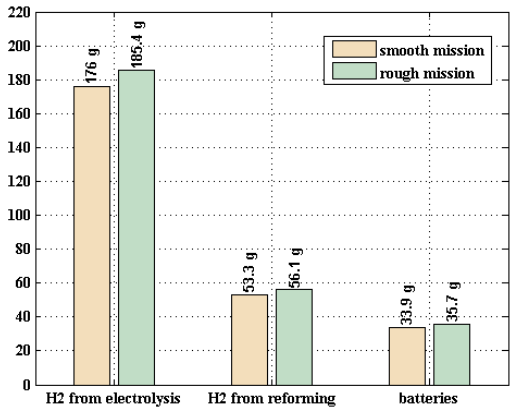

Figure 13 – Well-To-Wing emissions of carbon dioxide for the proposed powertrains in the Italian context

3 Increasing the energy content

For the initial value of stored energy content (1.9 MJ), the battery-based powertrain won over the fuel cell system. However, the result could be different if the energy content (and thus the endurance of the aircraft) was increased. To this, a suitable analysis was carried out by considering battery packs with different number of elements and fuel cell with different hydrogen capacity.

For the fuel cell case, the increase of energy stored on board was simulated with different approaches:

a) by increasing the number of fuel tanks, each with a capacity of 192SL;

b) by interpolating literature data to estimate the mass of the tank when increasing the capacity from 192SL to 993 SL.

In the second approach, the data provided by Linde S.r.l. [56] were used for the interpolation as shown in Figure 14.

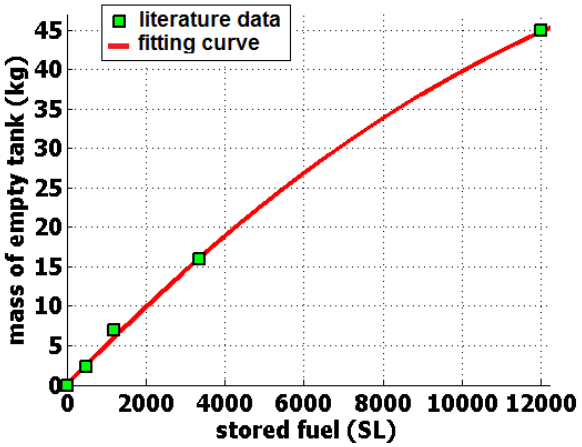

Figure 14 – Empty mass of hydrogen tanks versus stored fuel in Standard Liters (SL)

Accordingly, the number of battery elements in parallel was increased to match the energy content.

The increasing mass of the powertrain in both the battery-based and the fuel cell based powertrain would be so high as to require a re-design of the UAV. To take into account this

aspect, the empty mass and the wing area of the UAV were upgraded by keeping constant the ratios between total-to-empty mass and the total mass-to-wing area. The efficiency of the propeller and motor are assumed to be the same even if these components should be resized to account for the larger thrust request.

Since the largest differences between the fuel cell and the batteries were obtained on the max gross endurance, this parameter will be considered to drawn a threshold over which the fuel cell gives the best result. Moreover, this is easier to calculate with respect to the net endurance.

The results obtained with the two approaches are shown in Figure 15. The data of LiFePo4 are shown for completeness even if this battery could have been already excluded from the comparison.

In the case a) (more tanks) , the LiFP6 battery gives the largest endurance for all the values of the energy content. The LiPo battery and the fuel cell guarantee almost the same endurance for an energy content comprised between 6 and 10MJ.

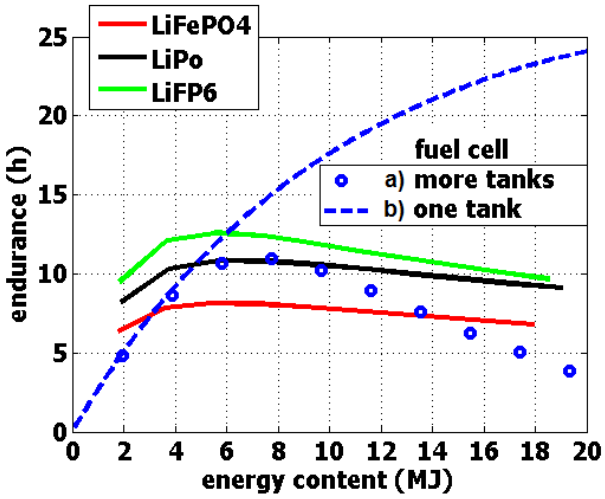

Figure 15 – Gross endurance vs energy content without changing empty mass and wing area

The use of a single tank with increasing capacity (case b) limits the increase of aircraft mass and makes the fuel cell GE become greater than the endurance of LiFP6 batteries when the energy content is over 5 MJ, as shown in Figure 15.

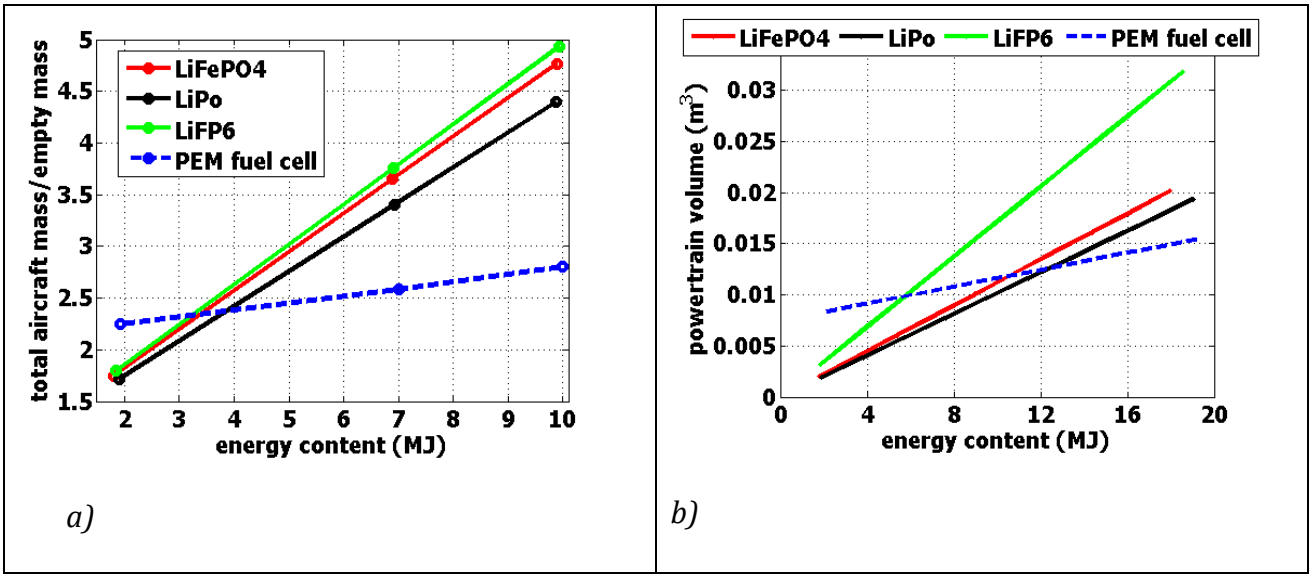

Figure 16 – Powertrain volume and aircraft mass to empty mass ratio vs energy content without changing empty mass and wing area

However, it is important to specify that this energy content is obtained by means of 39 LiFePO4 batteries, 34 LiPo batteries and 35 LiFP6 batteries. Accordingly, the total aircraft mass is 22.1 kg when it is powered by LiPo batteries, 23.8 kg in case of LiFP6 and 18.5 kg for the fuel cell. The increasing of the ratio of aircraft mass to empty mass with energy content is shown in Figure 16a for all the proposed powertrain while the volume occupied by the powertrain is in Figure 16b.

This means that the UAV needs to be redesigned to sustain the increased mass and volume of the powertrain when increasing the energy content. For this reason, a final case was considered by adjusting the empty mass and the wing area of the UAV with the energy content. To this, the ratios of aircraft mass to empty mass and wing area to aircraft mass were kept constant by adjusting the empty mass and the wing area. The resulting values of wing area and wing span are shown in Figure 17.

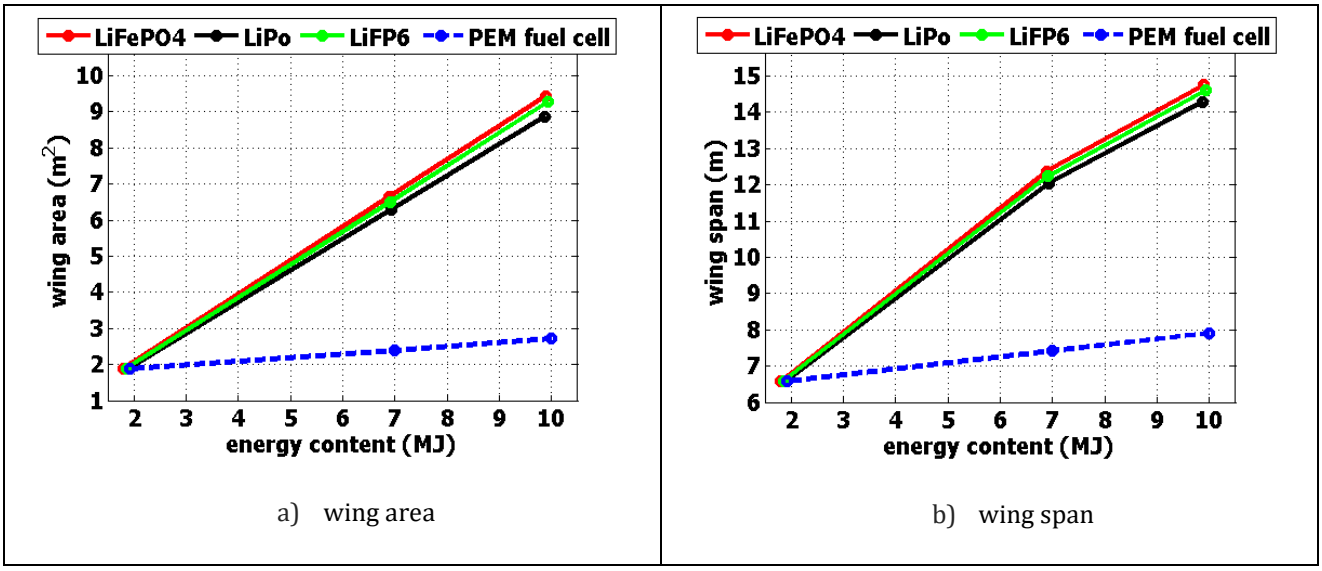

a) wing area

b) wing span

Figure 17 – Wing area and span vs energy content

The values of gross endurance for this last case are given in Figure 18. The fuel cell powertrain gives a higher endurance than all the battery configurations for an energy content higher than 4MJ. For this value of energy content, the empty mass and the wing specification in the case of fuel cell are very close to the initial values while in the case of LiFP6 battery, the empty mass and the wing area are about twice the initial values.

To further increase the endurance, it can be useful to consider hybrid propulsion systems using both batteries and hydrogen tanks as energy storage systems as proposed by [57].

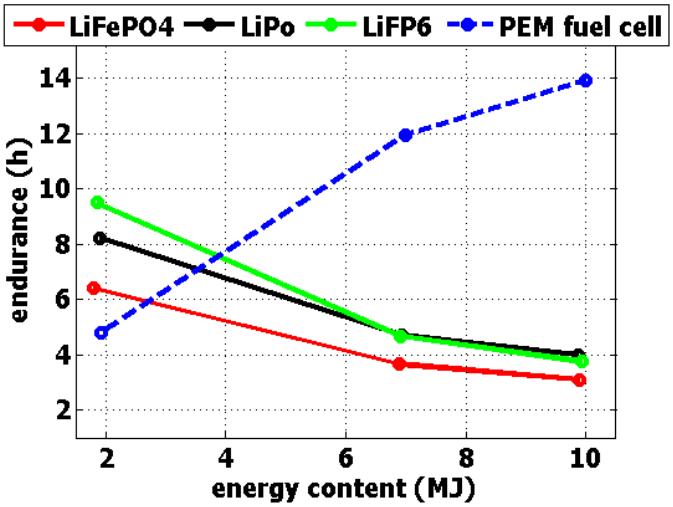

Figure 18 – Gross endurance vs energy content obtained by changing empty mass and wing area

4 Conclusions

The present investigation compared the performances of battery-based and fuel cell based powertrains for an all-electric unmanned aerial vehicle. LiFePO4, LiPo, LiFP6 battery technologies were examined for the purpose and the number of batteries in series and in parallel was chosen by matching the energy content of the hydrogen tank of the fuel cell-based powertrain.

The endurance was calculated using both a single point (gross endurance) and a mission based approach (net endurance). The gross endurance was evaluated with a correlation proposed in literature while the net endurance was obtained from the aircraft simulation model. The mission-based approach calculated hydrogen consumption or battery state of charge versus time along a pre-determined mission.

For the initial value of energy content (1.9MJ) the batteries proved to win the challenge because of the lower total mass required with respect to the fuel cell and, in particular, the LiFP6 technology was the best one in terms of max gross endurance and the LiPo won over the mission. The estimated well-to-wing environmental impact was also lower for the battery with the Italian electricity generation system.

The net endurance was found to be remarkably lower than the gross endurance for all powertrains. This justifies the approach of the authors (mission-based analysis) with respect to the simpler approaches used in literature. The effect of oscillations around the desired flight level and TAS was also quantified to have a more precise value of endurance for the proposed small UAV.

With the mission based approach, the difference of flight time between LiPo and LiFP6 technologies was very small. The flight time was sensibly lower in case of LiFePO4 batteries. This was due to the greater number of batteries and to the greater mass required to even the fuel cell energy content out when equipping the aircraft with LiFePO4 batteries.

The fuel cell powertrain performed better when increasing the amount of energy stored on board. Different hypotheses were formulated about the mass of the hydrogen tanks and of the whole aircraft when increasing the energy content. In the more realistic hypothesis, the fuel-cell-based powertrain gave the best results (highest gross endurance) for an energy content higher than 4MJ. This threshold value of energy content corresponds to a negligible increase of the aircraft empty mass, powertrain volume and wing area in the case of the fuel-cell powertrain while the aircraft needs to be redesigned in the case of the battery-based powertrains.

5 Acknowledgment

Investigation funded by the Italian Ministry for Education, University and Research (project code PON03_00067_8) and part of a research project of the Aerospace Technological District (DTA-Scarl).

6 References

[1] T. Price, D. Probert, Environmental Impacts of Air Traffic, Applied Energy, 50 (1996), pp. 133-162.

[2] H.A. Edwards, D. Dixon-Hardy , Z. Wadud, Aircraft cost index and the future of carbon emissions from air travel, Applied Energy 164 (2016) 553–562

[3] A.P. Roskilly, R. Palacin, J. Yan, Novel technologies and strategies for clean transport systems, Applied Energy, Volume 157, 1 November 2015, Pages 563-566, http://dx.doi.org/10.1016/j.apenergy.2015.09.051.

[4] Hadi Ebrahimi, Javad R. Gatabi, Hassan El-Kishky, An auxiliary power unit for advanced aircraft electric power systems, Electric Power Systems Research, Volume 119, February 2015, Pages 393-406

[5] J. W. Pratt, L. E. Klebanoff, K. Munoz-Ramos, A. A. Akhil, D. B. Curgus, B.L. Schenkman, Proton exchange membrane fuel cells for electrical power generation on-board commercial airplanes, Applied Energy, Volume 101, January 2013, Pages 776-796,

[6] A. Hoffrichter, P. Fisher, J. Tutcher, S. Hillmansen, C. Roberts, Performance evaluation of the hydrogen-powered prototype locomotive 'Hydrogen Pioneer', Journal of Power Sources, 250 (2014), pp. 120-127.

[7] BlueBird, Horizon unveil first commercial fuel cell UAV Fuel Cells Bulletin, Volume 2009, Issue 10, October 2009

[8] T. Kim, S. Kwon, Design and development of a fuel cell-powered small unmanned aircraft, International Journal of Hydrogen Energy, 37 (2012), 615-622

[9] G. Romeo, F. Borello, G. Correa, E. Cestino, ENFICA-FC: Design of transport aircraft powered by fuel cell & flight test of zero emission 2-seater aircraft powered by fuel cells fueled by hydrogen, International Journal of Hydrogen Energy, 38 (2013), 469-479

[10] F. Joseck, M. Wang, Y. Wu, Potential energy and greenhouse gas emission effects of hydrogen production from coke oven gas in U.S. steel mills, International Journal of Hydrogen Energy, 33 (2008), pp. 1445-1454.

[11] E. Cestino, Design of solar high altitude long endurance aircraft for multi payload & operations, Aerospace Science and Technology, 10 (2006), pp. 541-550.

[12] J.W. Pratt, L.E. Klebanoff, K. Munoz-Ramos, A.A. Akhil, D.B. Curgus, B.L. Schenkman, Proton exchange membrane fuel cells for electrical power generation on-board commercial airplanes, Applied Energy, 101 (2013), pp. 776-796.

[13] H.A. Gasteiger, J.E. Panels, S.G. Yan, Dependence of PEM fuel cell performance on catalyst loading, Journal of Power Sources, 127 (2004), pp. 162-171.

[14] P. Ramesh, M. Jithesh, Varun D., A novel system and technique for enhancing the lifetime of an air breathing micro PEM fuel cell based power source, IEEE International

System of Systems Engineering Conference (SoSE), 17-20 May 2015, San Antonio, TX, USA, pp. 128-133.

[15] A. Emadi, M. Ehsani, Aircraft power systems: technology, state of the art, and future trends, IEEE Aerospace and Electronic Systems Magazine, 15 (2000), pp. 28-32.

[16] N. Jenal, T.A. Ward, W. Kuntjoro, M.R. Aziz, N.V. David, A Study on Propeller Performance of a Fuel Cell Powered Propulsion System, IEEE International Conference on Control System, Computing and Engineering, 23-25 Nov. 2012, Penang, pp. 557-561.

[17] R. Peters, R.C. Samsun, Evaluation of multifunctional fuel cell systems in aviation using a multi-step process analysis methodology", Applied Energy, 111 (2013), pp 46-63.

[18] G.A. Whyatt, L.A. Chick, Electrical Generation for More-Electric Aircraft using Solid Oxide Fuel Cells, Department of Energy, (2012).

[19] T. Kim, S. Kwon, Design and development of a fuel cell-powered small unmanned aircraft, International Journal of Hydrogen Energy, 37 (2012), pp. 615-622.

[20] N. Lapeña-Rey, J. Mosquera, E. Bataller, F. Ortí, C. Dudfield, A. Orsillo, Environmentally friendly power sources for aerospace applications, Journal of Power Sources, 181 (2008), pp. 353-362.

[21] T.H. Bradley, B.A. Moffitt, D.N. Mavris, D.E. Parekh, Development and experimental characterization of a fuel cell powered aircraft, Journal of Power Sources, 171 (2007), pp. 793-801.

[22] M. Hepperle, Electric Flight - Potential and Limitations. Energy Efficient Technologies and Concepts of Operation, 22-24 October 2012, Lisbon, Portugal.

[23] D. Verstraete ,K. Lehmkuehler, A. Gong, J.R. Harvey, G. Brian, J.L. Palmer, Characterization of a hybrid, fuel-cell-based propulsion system for small unmanned aircraft, Journal of Power Sources 250 (2014) 204-211.

[24] D. A. Lawrence, and K., Mohseni., "Efficiency Analysis for Long-Duration Electric MAVs," Infotech@Aerospace 26 – 29 September 2005, Arlington, Virginia, AIAA 2005-7090.

[25] T. Chang, H. Yu, Improving Electric Powered UAVs' Endurance by Incorporating Battery Dumping Concept, Procedia Engineering 99 (2015), 168 – 179.

[26] McCormick B. W., Aerodynamics, Aeronautics and Flight Mechanics, John Wiley, 1995.

[27] Traub L. W., "Range and Endurance Estimates for Battery-Powered Aircraft", *Journal of Aircraft,* Vol. 48, No. 2, 2011.

[28] Traub L. W., "Validation of endurance estimates for battery powered UAVs", *Aeronautical Journal*, Vol. 117, No. 1197, 2013.

[29] G. Avanzini, F. Giulietti, Maximum Range for Battery-Powered Aircraft, Journal of Aircraft, 50 (2013), pp. 304-307.

[30] R. A. Fernandez, F. B. Cilleruelo, I. V. Martinez, A new approach to battery powered electric vehicles: A hydrogen fuel-cell-based range extender system, International Journal of Hydrogen Energy, Volume 41, Issue 8, 2 March 2016, Pages 4808-4819, http://dx.doi.org/10.1016/j.ijhydene.2016.01.035.

[31] J.Xu, B. Liu, X. Wang, D.Hu, Computational model of 18650 lithium-ion battery with coupled strain rate and SOC dependencies, Applied Energy, Volume 172, 15 June 2016, Pages 180-189, http://dx.doi.org/10.1016/j.apenergy.2016.03.108.

[32] A.Fotouhi, D. J.Auger, K. Propp , S. Longo, M. Wild , A review on electric vehicle battery modelling: From Lithium-ion toward Lithium–Sulphur, Renewable and Sustainable Energy Reviews, 56(2016)1008–1021.

[33] APC propeller web site, https://www.apcprop.com.

[34] Drive Calculator web site, http://www.drivecalc.de.

[35] Hacker motor web site, http://www.hacker-motor.com.

[36] A. Khaligh, L. Zhihao, Battery, Ultracapacitor, Fuel Cell, and Hybrid Energy Storage Systems for Electric, Hybrid Electric, Fuel Cell, and Plug-In Hybrid Electric Vehicles: State of the Art, IEEE Transactions on Vehicular Technology, 59 (2010), pp. 2806-2814.

[37] T. Donateo, M.G. De Giorgi, A. Ficarella, E. Argentieri, E. Rizzo, A General Platform for the Modeling and Optimization of Conventional and More Electric Aircraft, SAE 2014 Aerospace Systems and Technology Conference, pp. 1-11.

[38] T. Donateo, A. Ficarella, L. Spedicato, Development and validation of a software tool for complex aircraft powertrains, Advances in Engineering Software, 96 (2016), pp. 1-13.

[39] T. Donateo, L. Spedicato, M. Fedele, G. Trullo, A. Ficarella, Sizing and Simulation of a Piston-prop UAV, Proceeding of the 70th ATI Congress, Rome, 9-11 September, 2015.

[40] P. Panagiotou, P. Kaparos, C. Saplingidou, Yakinthos K., Aerodynamic design of a MALE-UAV, Aerospace Science and Technology, 50 (2016) pp. 127-138.

[41] G. de Carvahlo Bertoli, G. M. Pacheco, G. J. Adabo. Extending Flight Endurance of Electric Unmanned Aerial Vehicles through Photovoltaic System Integration, 4th International Conference on Renewable Energy Research and Applications, Palermo, Italy 22-25 Nov 2015.

[42] T. Donateo, D. Pacella, G. Indiveri, F. Ingrosso, A. Damiani, Dynamic Modeling of a PEM Fuel Cell for a Low Consumption Prototype, 2013 Technical SAE Paper, pp. 1-10.

[43] J. Benziger, E. Chia, J.F. Moxley, I.G. Kevrekidis, The dynamic response of PEM fuel cells to changes in load, Elsevier - Chemical Engineering Science, 60 (2005), pp. 1743-1759.

[44] O. Tremblay, L.-A Dessaint., A.I.,Dekkiche , A Generic Battery Model for the Dynamic Simulation of Hybrid Electric Vehicles, IEEE Vehicle Power and Propulsion Conference 0-7803-9761-4/07, 2007.

[45] O. Tremblay, L.-A Dessaint., Experimental Validation of a Battery Dynamic Model for EV applications, World Electric Vehicle Journal Vol. 3, 2009.

[46] A. Hausmann, C. Depcik, Expanding the Peukert equation for battery capacity modeling through inclusion of a temperature dependency, Journal of Power Sources, 235 (2013), pp. 148-158.

[47] A. Arista, M. Ferraro, F. Sergi, V. Antonucci, Dynamic Model of High-Performance Li-ion cells (LiFePO4, Li-Polymers and LiFP6 NBC) in different load conditions, 6th IC-EpsMsO, Athene, 2015, ISSN: 2241-9209.

[48] Y. Su, H. Liahng, J. Wu, Multilevel Peukert Equations Based Residual Capacity Estimation Method for Lead-Acid Batteries, IEEE International Conference on Sustainable Energy Technologies, IEEE Publ., 2008, Piscataway, NJ, pp. 101-105.

[49] V. Pop, H.J. Bergveld, P.H.L. Notten, P.P.L. Regtien, State-of-the-art of battery state-of-charge determination, in: Battery Management Systems, Springer Netherlands, pp. 11-45.

[50] S. Piller, M. Perrin, A. Jossen, Methods for state-of-charge determination and their applications, Journal of Power Sources, 96 (2001), pp. 113-120.

[51] Kong Soon Ng, Chin-Sien Moo, Yi-Ping Chen, Yao-Ching Hsieh, Enhanced Coulomb counting method for estimating state-of-charge and state-of-health of lithium-ion batteries, Applied Energy, 86 (2009), pp. 1506-1511.

[52] CO_2 Emissions from Fuel Combustion, Annual Report, International Energy Agency (IEA), 2014.

[53] D. Bonaquist, Analysis of CO_2 Emissions, Reductions, and Capture for Large-Scale hHydrogen Production Plants, Praxair white paper 2010, pp. 1-9.

[54] S. Eaves, J. Eaves, A cost comparison of fuel-cell and battery electric vehicles, Journal of Power Sources 130 (2004) 208–212

[55] A. Vasan, B. Sood, M. Pecht, Carbon footprinting of electronic products, Applied Energy 136 (2014) 636–648

[56] Linde Gas Italia, private communication, February 2016.

[57] R.O. Stroman, M. W. Schuette, K. Swider-Lyons, J. A. Rodgers, D.J. Edwards, Liquid hydrogen fuel system design and demonstration in a small long endurance air vehicle, International Journal of Hydrogen Energy, Volume 39, Issue 21, 15 July 2014, Pages 11279-11290, http://dx.doi.org/10.1016/j.ijhydene.2014.05.065.